Talanta xxx (xxxx) xxxx

Contents lists available at ScienceDirect

Talanta

journal homepage: www.elsevier.com/locate/talanta

Paper-based colorimetric spot test utilizing smartphone sensing for detection of biomarkers

Eda Aydindogan[a], Ayse Elcin Ceylan[a], Suna Timur[a,b,*]

[a] Ege University, Institute of Natural Sciences, Department of Biochemistry, 35100, Bornova, Izmir, Turkey
[b] Central Research Testing and Analysis Laboratory Research and Application Center, Ege University, 35100, Bornova, Izmir, Turkey

ARTICLE INFO

Keywords:
Paper-based
Colorimetric
Spot test
Biosensor
Cancer
Biomarker
Alpha-fetoprotein
Mucin-16

ABSTRACT

The need for a continuous, real-time monitoring of specific diseases represents an unmet scientific need. Evidently, cancer is one of the most important diseases where it is crucial to increase the rates of patient survival and monitor disease prognosis. Herein, a novel type of immunoassay was developed for detection of cancer biomarkers, using alpha-fetoprotein (AFP) and mucin-16 (MUC16) as model analytes. Using gold nanoparticle (AuNP) bioconjugates as a signal production tool, relevant antibody (Ab)-conjugated AuNPs were prepared on the nitrocellulose (NC) membrane. To construct a spot-like point-of-care (POC) immunoassay, cysteamine conjugated AuNPs (AuNP-Cys) were immobilized on the NC membrane and antibodies were conjugated to the nanoparticle on the detection pad, following a treatment with the samples that contains AFP or MUC16 which are well-known protein biomarkers for liver and ovarian cancer. By using the change in the colorimetric properties of AuNPs, detection of tumor markers was achieved by using a smartphone image and color analysis software at the final stage. Image J application was used for the evaluation of color changes depending on the biomarker concentration in buffer or spiked synthetic serum samples. The linear range was found as 0.1 ng/mL-100 ng/mL for AFP and 0.1–10 ng/mL for MUC16. Limit-of-detection (LOD) was calculated as 1.054 ng/mL and 0.413 ng/mL for AFP and MUC16, respectively. Interferent molecules, Her2, Immunoglobulin G (IgG) and bovine serum albumin (BSA) were tested on the system. Furthermore, synthetic serum samples spiked with selected analyte molecule were applied on the system and measured successfully.

1. Introduction

In the age of information, healthcare technology has recently been shifting from centralized medical laboratories to point-of-care (POC) diagnostic devices with the development of micro and nano technology, cloud computing, advances in signal processing and microelectronics. The need for a continuous, real-time monitoring of a specific health condition drives the motivation to reduce the gap between the availability of healthcare facilities and the demand especially in developing countries due to inadequate healthcare budgets [1,2]. The next generation POC platforms focuses on the development of affordable, sensitive and specific, user-friendly, rapid and robust, equipment-free, and deliverable to those in need, namely 'ASSURRED' technologies to be enabled in diagnostic analysis and other clinical applications [3]. Compared to laboratory-based analyses, POC gives rapid and accurate results without being costly. Accordingly, it is a preferable alternative especially in resource-limited areas to reduce disease morbidity and mortality and consequently, to improve the overall quality of life [4].

Even though there are a number of POC systems developed in the last decade, most of them has either not been commercialized or widely established in the market due to the lack of integration and automation of the designs [5]. Both to automate and integrate the POC diagnostics to medical world, smartphone technology emerges as the most obvious choice. According to statistics, the number of smartphone users is predicted to grow from 2.1 billion in 2016 to around 2.87 billion in 2020 [6]. Smartphones are fully equipped with high-resolution cameras, powerful processors, wireless connectivity, real-time analysis abilities, secure data management, and cloud computing [7]. Most of these properties have become useable in healthcare through the applications, or "apps" that can analyze the signal out-comes acting as an interface or the sensor itself [8,9]. There emerges a term 'mobile health (mHealth)' referring to the relationship and data sharing between patients and doctors which transformed into sending and sharing calls, text messages and personal information via websites and/or applications [10,11]. mHealth aims to provide an immediate resource for clinical decision by the healthcare professionals, prescription

* Corresponding author. Ege University, Institute of Natural Sciences, Department of Biochemistry, 35100, Bornova, Izmir, Turkey.
E-mail addresses: edacelikbas@ku.edu.tr (E. Aydindogan), elcinceylan5@gmail.com (A.E. Ceylan), sunatimur@yahoo.com (S. Timur).

https://doi.org/10.1016/j.talanta.2019.120446
Received 12 August 2019; Received in revised form 1 October 2019; Accepted 4 October 2019

information and other medical treatments for a better personalized healthcare [12,13]. Thus, at this rate of usage and with so many beneficial properties, smartphones are the prominent alternative to complicated and expensive laboratory devices which requires more time and effort to provide reliable results.

Smartphones have been widely used in biosensing assays, as detectors, data processors, and even signal inducers with small additional devices [14–17]. Many biological molecules such as enzymes [18,19], cells [20,21], nucleic acids [22,23], antigen–antibodies [24,25], and microorganisms [2,26] can be tested using smartphones. High-quality camera lenses on smartphones play a crucial role and are adapted extensively for optical biosensor designs. By using the cameras as a 'smart detector', complementary metal oxide semiconductor (CMOS) image sensors as a 'smart recorder' and specific applications (apps) as 'smart readout', almost all the optical-based testing methods such as imaging, absorbance, reflectance, fluorescence, surface plasmon resonance (SPR), localized surface plasmon resonance (LSPR), bio-chemiluminescence and electrochemiluminescence can be integrated with smartphone technology [27]. Yet, majority of the recent literature on optical smartphone biosensing focuses on the POC platforms that use colorimetric or fluorescence-based measurement principles due to simplicity of the designs and the analysis [24,28–30]. Colorimetric assays measure the changes in the absorbance or reflectance intensity of conjugates, whereas, fluorescence-based assays detect the light emitted from the target sample upon radiative excitation [31,32]. Color intensity-based smartphone sensing platforms mostly involve an evaluation of color changes as the final result in an assay which is either based on immune complex formation or a specific chemical reaction. CMOS image sensors collects the optical signal, uses an algorithm, via apps, to process the images captured by the CMOS detector [33]. As a result, one can simply observe the testing outcomes on the screen of the smartphone.

The current literature in the context of smartphone-based biomarker detection leads in lateral flow assays [34], microarray chips [25], μwell-based methods [35–37] and electrochemical techniques [38]. A few studies show that a more practical approach is possible using spot-like modules on paper for the analysis [10,39,40]. Herein, we developed a novel spot-like paper-based assay using AuNP bioconjugates as color provider and commercially available cancer biomarkers as the analyte of interest. AuNPs are conjugated with Cys molecules using gold-thiol affinity and immobilized on the NC membrane. After the immobilization of the *anti*-AFP or *anti*-MUC16 antibodies on the surface via glutaraldehyde (GA), different concentrations of AFP or MUC16 solutions are added to the spots on the NC membrane and the color change on the AuNP surface is analyzed using smartphone images via Image J software. The proposed design is given in Scheme 1. The range of analysis and the linear range for this method is found as 0.1 ng/mL-1.0 μg/mL and 0.1–100 ng/mL, respectively for AFP analysis. The same analytical values were calculated as 0.1–50 ng/mL and 0.1–10 ng/mL for MUC16, respectively. It is also shown that this method can be used in the existence of interferant molecules and this platform is successfully measuring AFP and MUC16 in serum samples which previously spiked with known concentrations of the analyte.

2. Material and methods

2.1. Materials

Bovine serum albumin (BSA), cysteamine hydrochloride (≥%97.0), glutaraldehyde (Grade II, 25%) *anti*-AFP and *anti*-MUC16 Antibodies (Prestige Antibodies) and AFP, MUC16 and Her2 Antigens (Prestige Antigens) were pur-chased from, Sigma-Aldrich (St Louis, USA). Nitrocellulose (NC) membrane was obtained from mdi Membrane Technologies (Ambala Cantt 133 006, India). 40 nm Standard Gold Nanoparticles were obtained from Cytodiagnostics (Ontario, Canada). All other chemicals were rea-gent grade.

2.2. Instruments

Mini thermal shaker (Biosan TS-100C Thermo Shaker) and microliter centrifuge (Hettich) were used for the AuNP-Cys conjugation procedure. For the characterization of the particles, size and zeta potential measurements were carried out with dynamic light scattering (DLS) (Malvern Zetasizer, NanoZS Model, Malvern Instruments Ltd., UK) method. For the colorimetric analysis, all photographs were taken during the sunlight using an Apple iPhone 7 without any flashlight. All photographs were analyzed using the Image J software, using the weighted color intensity values. For the UV–Vis absorbance measurements, Thermo Fisher Scientific NanoDrop ONE device was used.

2.3. AuNP-Cys conjugation

AuNP-Cys conjugation was performed according to a previously reported method [41]. Briefly, 5.0 μL of 1.0 μg/mL Cys was added to 2.0 mL AuNP solution from the stock. The solution was incubated at 1000 rpm, 25 °C for 2 h. After the incubation, the solution was centrifuged at 3000 rpm, 4 °C for 20 min. Unreacted cysteamine was then dis-carded as the supernatant and the pellet was washed with sodium phosphate buffer (10 mM, pH 7.4) two times. Final supernatant was discarded, and the volume was completed to 300 μL with sodium phosphate buffer (10 mM, pH 7.4).

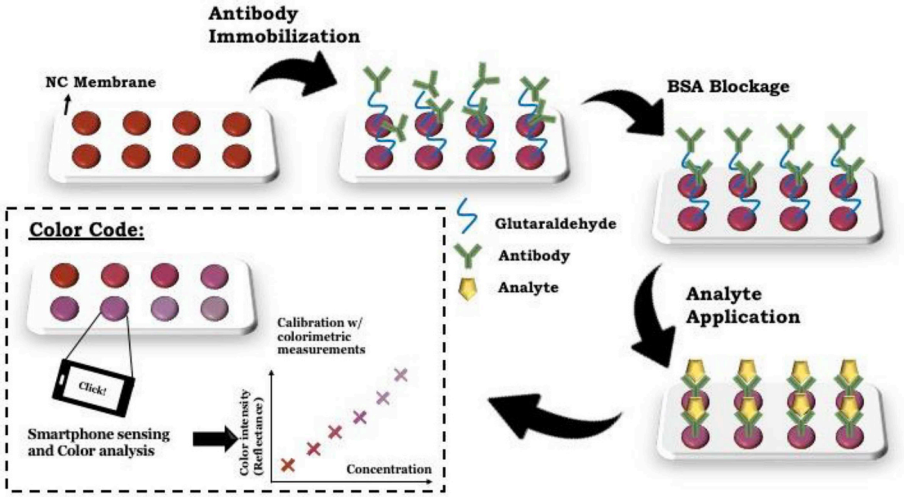

Scheme 1. Schematic illustration of the proposed spot-like POC testing design.

2.4. Design of the NC membrane

In this work, a paper-based colorimetric method was developed using smartphone sensing as illustrated in Scheme 1. The protocol involves the following steps: a) spotting the AuNP-Cys solution on NC membrane; b) Ab immobilization using amine chemistry; c) blocking step; and d) reaction with antigens. The spots on the NC membrane are prepared freshly for every experiment. First of all, the membrane was pretreated with 10 mg/mL BSA solution to facilitate the formation of a circular shape as a 'spot-like' platform. It has been observed that, without the pretreatment, the movement of the AuNP-Cys particles were not limited and they spread on the whole membrane, without forming any particular shape. 2.0 μL of AuNP-Cys conjugates were dropped on the pretreated NC membrane and dried for 30 min at ambient conditions. After the formation of the spots, 1.0 μL of 20 μg/mL antibodies, either *anti*-AFP or *anti*-MUC16, were immobilized on the surface using 1.0 μL 1.0% GA as a crosslinker. The antibody amount immobilized on the surface was determined according to the similar work previously conducted by Hosu et al. [10]. The spots were allowed to react for 30 min at ambient conditions. Unreacted components were discarded by washing the spots thoroughly with 10 mM sodium phosphate buffer and allowed to dry. The membrane was then blocked with 1.0 mg/mL BSA solution to eliminate the effect of nonspecific adsorption and allowed to dry again. Finally, 10 μL of different concentrations of relevant analyte solutions were dropped on the spots and incubated for another 30 min at ambient conditions. Unbound molecules were removed by washing with 10 mM sodium phosphate buffer again and allowed to dry for the color analysis. Additional control experiments, antibody immobilization confirmation, incubation time optimization and stability control of the proposed platform, were conducted following the same experimental steps.

2.5. Smartphone-based colorimetric analysis

Images were taken in a well-lit room during the day, with-out any external light source or flash, with an Apple iPhone 7 device. After each step of the analysis, AuNP-Cys spots, AuNP-Cys/Ab spots and AuNP-Cys/Ab/Analyte spots, photographs of the NC membrane were captured and analyzed using Image J software. The spots were cut individually for analysis using the software's image editing tools and the histogram of the colors on that particular spot was acquired. Experimental steps for the image analysis are presented in Scheme 2. For the clarity and simplicity of the experiment, weighted color intensity values were used for the analysis.

3. Results and discussion

Development of a simple, low-cost, practical and user-friendly detection platforms for biomarkers is of great importance for both POC diagnostics and mHealth area. This study proves that there are simple alternatives to the systems in the literature which are rather complex and requires external devices for the analysis.

The hydrodynamic particle sizes of AuNP-Cys conjugates were estimated via DLS method and ζ potential measurements were conducted and the results were presented in Table 1. According to size measurements, AuNPs presented a size of 31.53 ± 8.84 nm, close as given in manufacturer's instructions. After the conjugation, particle size increased to 38.01 ± 11.08 nm and confirmed a successful bonding of the Cys group onto AuNP surface. Additionally, the low polydispersity index (PDI) illustrates the homogeneity of the particles in the solution. Furthermore, ζ potential measurements were also confirmatory for the conjugation. Prior to Cys conjugation, surface potential of the AuNPs were measured as −33.2 mV, afterwards increasing to −28.6 mV, confirming the increase of positively charged amine groups on the surface.

It is well known that nanosized metal particles exhibit strong absorption bands in the visible region of the spectrum. Specifically, AuNPs has a wine-red coloring due to the Mie absorption by their surface plasmon resonance peaks at 520 nm [42]. The size and shape of the nanoparticles affect this absorption peak. An increase in size leads to a red-shift to the longer wavelengths in absorbance due to the electric dipole-dipole interactions between the neighboring particles [43]. As the interparticle distance between AuNPs decreases (i.e. antibody or analyte conjugation) to less than the average particle diameter, the color of the solution starts to shift blue [44]. Fig. 1A represents the calibration curve obtained for AFP detection with the proposed method. Different concentrations of analytes in the range of 0.01 ng/mL – 1.0 μg/mL were dropped onto the AuNP-Cys/*Anti*-AFP modified spots on the NC membrane and the results were monitored by capturing the images of the spots. Each spot was cropped separately and processed using an image analysis application. Using the difference in color intensity values between AuNP-Cys/*Anti*-AFP and AuNP-Cys/*Anti*-AFP/AFP modified spots, a good linear correlation was observed in a broad range between 0.1 and 100 ng/mL. Similarly, for the MUC16 analysis, MUC16 solutions in between the range 0.1–100 ng/mL were applied to the AuNP-Cys/*Anti*-MUC16 modified spots on the membrane. Using the same analytical values, a good linear range of 0.1–10 ng/mL was obtained (Fig. 1B).

Experimental conditions were verified in terms of antibody immobilization, incubation time and sensor stability. A control experiment was conducted to confirm the successful immobilization of the antibody on the surface. For these experiments *anti*-AFP antibody solution and AFP analyte solution was used. After the immobilization of the AuNP-Cys on the surface, spots were prepared using the same amount of buffer solution instead of antibody solution to conduct a comparison experiment if there is a difference in the signal change with the antibody immobilization. As shown in Fig. 2A, when the analyte solutions were added on the spots (100 and 500 ng/mL AFP solutions), the signal difference was decreased more than 50% when no antibodies were immobilized on the AuNP-Cys modified spots on NC membrane. The results were confirming a successful immobilization of the antibodies on the surface. Antibodies were immobilized on the AuNP-Cys modified spots, rather than performing the conjugation in solution phase, to better observe and follow the changes on the modification of the surface. Additionally, when covalently bound on the surface, orientation of the antibody is known to provide the best recognition conditions [45,46].

Incubation time was optimized using the same principle for preparing the spots, changing the time for reaction. After dropping the samples on the NC membrane for each step, AuNP-Cys, AuNP-Cys/Ab and AuNP-Cys/Ab/An, reactions were monitored by capturing the images of the colors for 15, 30, 45, 60 min intervals and the results were presented in Fig. 2B. The color intensity of the images measured with the Image J software represents the reflected light, which is the visible light, from the spots under the ambient lighting conditions in red, green, blue (RGB) space [47]. The results indicated that at the 30 min threshold of incubation, the reflected light intensity is at the maximum, meaning that the absorbed light intensity is at the minimum. The absorbance values of AuNPs decrease with the conjugation and incubation time [48,49]. Thus, the experimental results confirmed that the optimal incubation time for the maximum absorbance values is 30 min.

Sensor stability was monitored over the course of five days, using the AuNP-Cys/Ab modified surface in different conditions. This surface was chosen for its potential commercial application because this would be the step where it would be appropriate to procure the spot-test system as in commercial pregnancy test kits where only analyte is applied afterwards. The tests were kept in both room temperature and 4 °C to observe the stability of the system in different conditions. As can be seen in the results presented in Fig. 2C, after the 4th day, the consistency and integrity of the designed platform decayed and a higher reflectance (i.e. lower absorbance) values were obtained. As explained in previously, the absorption band of AuNPs shifts to longer

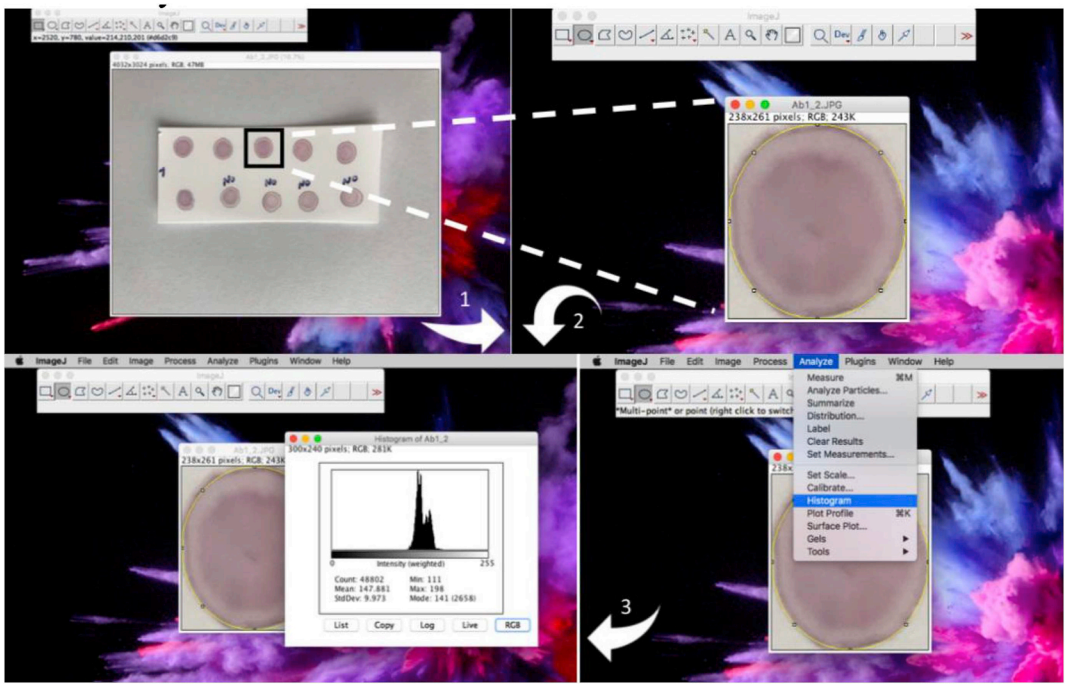

Scheme 2. Analysis steps for the colorimetric measurements of the smartphone images via Image J software.

Table 1
Results of DLS and zeta potential measurements performed to characterize AuNP-Cys conjugates.

	Size (nm) ± SD	PDI	ϛ Potential (mV) ± SD
AuNP	31.53 ∓ 8.84	0.158	−33.2 ∓ 8.41
AuNP-Cys	38.01 ∓ 11.08	0.106	−28.6 ∓ 9.69

± SD values were obtained from three independent measurements of freshly prepared samples.

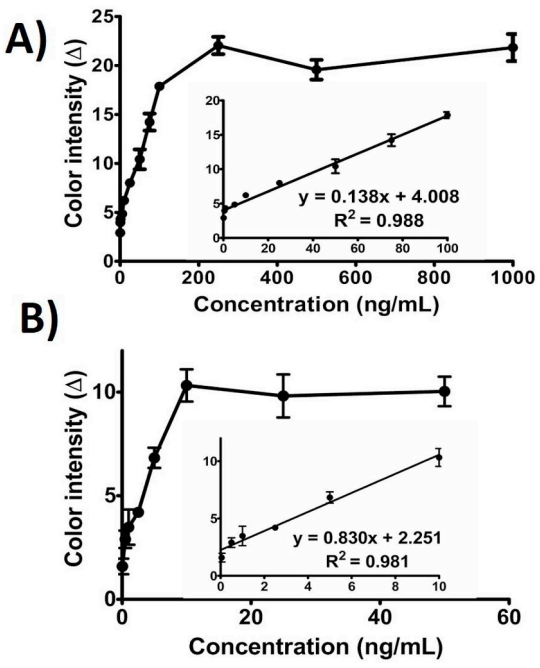

Fig. 1. Calibration curve from a smartphone-based detection of color intensity differences for A) AFP and B) MUC16 [error bars show ± S.D].

wavelengths with size and incubation time, thus, it can be concluded that the proposed sensing platform was stable over the course of 4 days.

Various analytical parameters for the experiment were calculated to determine the performance of the designed platform for detecting biomarkers successfully and presented in Table 2. The repeatability of the experiment was deter-mined with ten spots at 25 ng/mL concentration as it is the middle point of the linear range. Repeatability (± S.D.) was calculated as 0.044 and 0.215 for AFP and MUC16, respectively. Coefficient of variation (CV) was calculated as 0.549% and 2.697% for AFP and MUC16, respectively, using the ((± S.D./Average)*100) formula. Additionally, with the ((3.3* ± S.D.)/Slope) formula, LOD values were calculated. For AFP, LOD was calculated as 1.054 ng/mL and for MUC16 it was obtained as 0.413 ng/mL. The literature cut-off value for AFP is reported as 20 ng/mL [50], thus, designed platform was considered remarkable in determining a low value of protein levels in buffer solutions. As for the MUC16, which is the synonym for CA125; a well-known ovarian cancer biomarker, the literature cut-off value is reported as 35 U/mL [51]. As we used a commercially available antigen solutions for the experiments, which has a main stock concentration values in mg/mL, there is no available literature which can be compared to our experimental results.

The selectivity of the proposed platform was tested with possible interfering molecules selected. After the immobilization of antibodies on the surface, different interferant molecules at the same concentration rate was dropped on the spots. For *anti*-AFP antibodies on the surface, 25 ng/mL Her2, MUC16, IgG and BSA solutions were used as interfering molecules. As for the *anti*-MUC16 antibodies, 1.0 ng/mL Her2, AFP, IgG and BSA solutions were selected as interferants. Her2, AFP and MUC16 were selected as they are some other protein biomarkers for a different cancer and IgG and BSA were selected for their possibility of availability in biological matrices. Relative response signals were calculated with respect to the response for AFP and MUC16 as 100%. As shown in Fig. 3A and B, the proposed colorimetric platform did not respond significantly to the other interferants, indicating a high selectivity for AFP and MUC16, respectively.

Finally, to determine the biological matrix applicability, synthetic serum samples spiked with AFP or MUC16 solutions at different concentrations were applied to spots which were modified with AuNP-Cys/

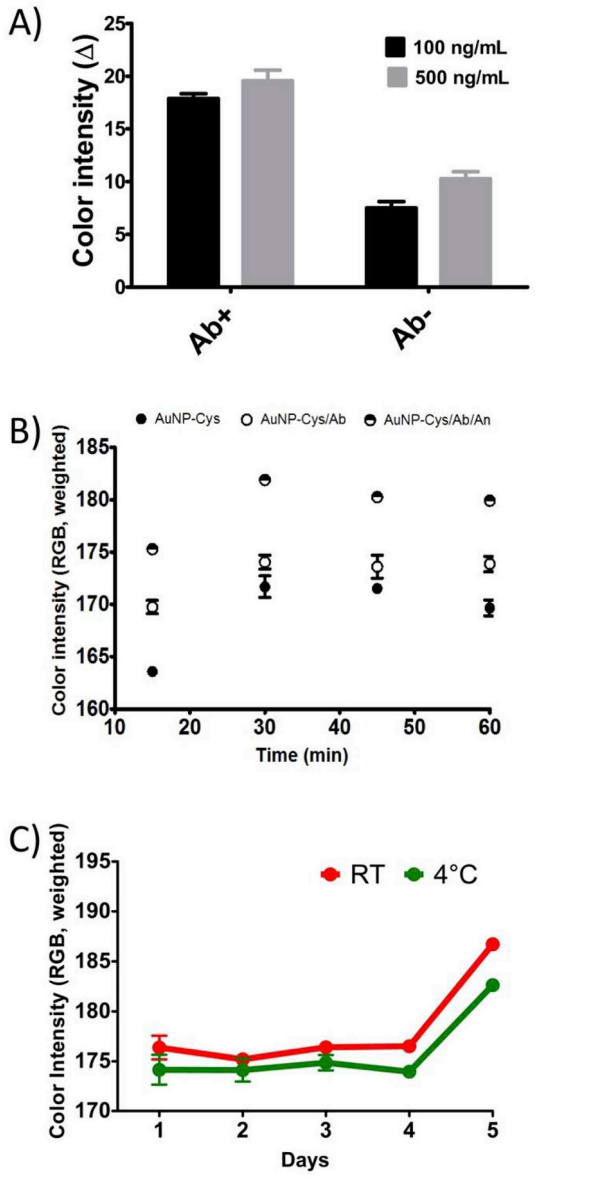

Fig. 2. Optimization of experimental conditions; A) Antibody immobilization confirmation experiments conducted by using the same amount of buffer solution instead of antibody solution [Ab+: presence of antibodies, Ab-: absence of antibodies] B) Optimization of incubation time for the experiment, using the RGB color intensity (weighted) values from Image J software and C) The stability of the proposed spot-test system in different conditions [error bars show ± S.D]. (For interpretation of the references to color in this figure legend, the reader is referred to the Web version of this article.)

Anti-AFP or AuNP-Cys/*Anti*-MUC16 on NC membrane and the color intensity differences in test spots were analyzed by Image J software. It has been reported that both AFP and MUC16 levels are measured in serum samples in clinical practice [52,53]. As presented in Table 3, the amount of AFP in synthetic serum samples which were spiked with 10 and 25 ng/mL AFP solutions were measured as 10.045 and 23.980 ng/mL, respectively, with a high recovery rate. Similarly, the MUC16 levels in the serum samples spiked with 1.0 and 5.0 ng/mL MUC16 solutions were detected as 0.94 and 4.86 ng/mL. All relative standard deviation (RSD) values were under 5%. These results were clearly supporting the potential use of the proposed method for POC detection of protein biomarkers for cancer.

Table 2
Analytical characteristics for the developed colorimetric smartphone sensing platform.

Analytical Parameters	Values	
	AFP	MUC16
Linear Range (ng/mL)	0.1–100	0.1–10
Slope	0.137	0.830
Intercept	4.008	2.251
± S.D. of intercept	0.262	0.272
± S.D. of slope	0.005	0.058
Correlation coefficient	0.988	0.981
Limit of detection (LOD; ng/mL)	1.054	0.413
Reproducibility (± S.D.)	0.044	0.215
Coefficient of variation	0.549%	2.697%

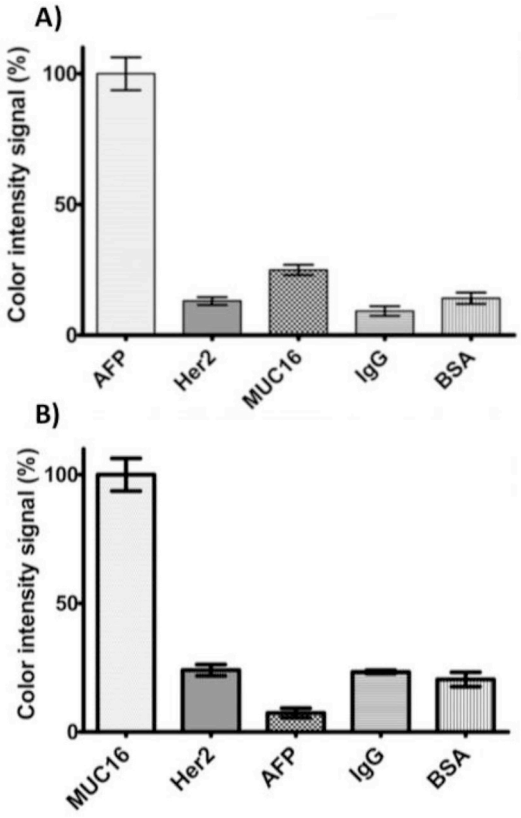

Fig. 3. Effect of various interfering molecules such as MUC16, AFP, Her2, IgG, BSA. The response signals were obtained with color intensity (weighted) values with respect to the signals corresponding to relevant antibody on the surface. [All experiments were the same as mentioned before, error bars show ± S.D].

Table 3
Sample application results using the spiked synthetic serum samples measured with the smartphone sensing platform.

AFP			
Spiked AFP (ng/mL)	Measured AFP (ng/mL)	Recovery (%)	RSD
10	10.04	100.45	3.17
25	23.98	95.92	1.59
MUC16			
Spiked MUC16 (ng/mL)	Measured MUC16 (ng/mL)	Recovery (%)	RSD
1.0	0.94	94.18	0.23
5.0	4.86	97.29	4.12

4. Conclusions

In conclusion, we present a novel, simple, rapid, sensitive and specific platform that can be potentially used for the analysis of protein biomarkers for various diseases. In this study, AFP and MUC16 biomarkers, which are the known markers of hepatocellular carcinoma (liver cancer) and ovarian cancer, respectively, were selected as model analytes as POC cancer diagnostics are in parallel with an unmet need all over the world. The proposed biosensing system was successfully used for the analysis of AFP and MUC16 in synthetic serum samples. Furthermore, potential interfering molecules were tested on the system and it has been shown that the proposed method enables a specific analysis of the desired analytes.

The most important drawback of the lateral flow immunoassays, which is the so-called rival platform for this study, is cross-reactivity and the uncontrollable capillary force of the membrane [54]. Additionally, lateral flow assays require the combination of many different membranes in the correct form and the construction process require the consideration of many different parameters [55]. Cross-reactivity is avoided by dropping the analyte solution only on the spots that contains the relevant antibody and the unwanted capillary action is prevented by the circle-like nature of the designed spots. With the development of a spot-like assay on a single NC membrane without any further modifications, a simpler and more practical approach is proposed [10]. All presented data holds great potential for the further work using low-cost, spot-like systems on paper utilizing smartphone-sensing technology for different molecules of interest.

Author contributions

The manuscript was written through contributions of all authors. All authors have given approval to the final version of the manuscript. The authors declare no competing financial interest.

Acknowledgment

This work was supported by a COST project of Scientific and Technological Research Council of Turkey (TUBITAK, Project Grant No: 117Z609).

References

[1] R.S. Khan, Z. Khurshid, F. Yahya Ibrahim Asiri, Advancing point-of-care (PoC) testing using human saliva as liquid biopsy, Diagnostics (2017) 7.
[2] Q. Wei, H. Qi, W. Luo, D. Tseng, S.J. Ki, Z. Wan, et al., Fluorescent imaging of single nanoparticles and viruses on a smart phone, ACS Nano 7 (2013) 9147–9155.
[3] D. Mabey, R.W. Peeling, A. Ustianowski, M.D. Perkins, Diagnostics for the developing world, Nat. Rev. Microbiol. 2 (2004) 231–240.
[4] M. Urdea, L.A. Penny, S.S. Olmsted, M.Y. Giovanni, P. Kaspar, A. Shepherd, et al., Requirements for high impact diagnostics in the developing world, Nature 444 (Suppl 1) (2006) 73–79.
[5] P.K. Drain, E.P. Hyle, F. Noubary, K.A. Freedberg, D. Wilson, W.R. Bishai, et al., Diagnostic point-of-care tests in resource-limited settings, Lancet Infect. Dis. 14 (2014) 239–249.
[6] T.S.P. Statista, Smartphone Users Worldwide 2014-2020, (2019).
[7] Y. Wang, Y. Li, X. Bao, J. Han, J. Xia, X. Tian, et al., A smartphone-based colorimetric reader coupled with a remote server for rapid on-site catechols analysis, Talanta 160 (2016) 194–204.
[8] D. Gallegos, K.D. Long, H. Yu, P.P. Clark, Y. Lin, S. George, et al., Label-free biodetection using a smartphone, Lab Chip 13 (2013) 2124–2132.
[9] J.L. Delaney, E.H. Doeven, A.J. Harsant, C.F. Hogan, Use of a mobile phone for potentiostatic control with low cost paper-based microfluidic sensors, Anal. Chim. Acta 790 (2013) 56–60.
[10] O. Hosu, A. Ravalli, G.M. Lo Piccolo, C. Cristea, R. Sandulescu, G. Marrazza, Smartphone-based immunosensor for CA125 detection, Talanta 166 (2017) 234–240.
[11] B. Martínez-Pérez, I. de la Torre-Díez, M. López-Coronado, Mobile health applications for the most prevalent conditions by the World health organization: review and analysis, J. Med. Internet Res. 15 (2013) e120.
[12] W. Wiechmann, D. Kwan, A. Bokarius, S.L. Toohey, There's an app for that? Highlighting the difficulty in finding clinically relevant smartphone applications, West. J. Emerg. Med. 17 (2016) 191–194.
[13] H. Oh, C. Rizo, M. Enkin, A. Jadad, What is eHealth (3): a systematic review of published definitions, J. Med. Internet Res. 7 (2005) e1.
[14] X. Meng, H. Huang, K. Yan, X. Tian, W. Yu, H. Cui, et al., Smartphone based hand-held quantitative phase microscope using the transport of intensity equation method, Lab Chip 17 (2017) 104–109.
[15] D. Calabria, C. Caliceti, M. Zangheri, M. Mirasoli, P. Simoni, A. Roda, Smartphone-based enzymatic biosensor for oral fluid L-lactate detection in one minute using confined multilayer paper reflectometry, Biosens. Bioelectron. 94 (2017) 124–130.
[16] J.-S. Yang, J. Shin, S. Choi, H.-I. Jung, Smartphone Diagnostics Unit (SDU) for the assessment of human stress and inflammation level assisted by biomarker ink, fountain pen, and origami holder for strip biosensor, Sens. Actuators B Chem. 241 (2017) 80–84.
[17] J. Liu, Z. Geng, Z. Fan, J. Liu, H. Chen, Point-of-care testing based on smartphone: the current state-of-the-art (2017-2018), Biosens. Bioelectron. 132 (2019) 17–37.
[18] N. Alizadeh, A. Salimi, R. Hallaj, Mimicking peroxidase-like activity of Co3O4-CeO2 nanosheets integrated paper-based analytical devices for detection of glucose with smartphone, Sens. Actuators B Chem. 288 (2019) 44–52.
[19] A.J. Bandodkar, S. Imani, R. Nuñez-Flores, R. Kumar, C. Wang, A.M.V. Mohan, et al., Re-useable electrochemical glucose sensors integrated into a smartphone platform, Biosens. Bioelectron. 101 (2018) 181–187.
[20] X. Wang, G. Lin, G. Cui, X. Zhou, G.L. Liu, White blood cell counting on smartphone paper electrochemical sensor, Biosens. Bioelectron. 90 (2017) 549–557.
[21] Y. Zeng, K. Jin, J. Li, J. Liu, J. Li, T. Li, et al., A low cost and portable smartphone microscopic device for cell counting, Sens. Actuators A Phys. 274 (2018) 57–63.
[22] X. Xu, X. Wang, J. Hu, Y. Gong, L. Wang, W. Zhou, et al., A smartphone-based on-site nucleic acid testing platform at point-of-care settings, Electrophoresis 40 (2019) 914–921.
[23] C.F. Fronczek, T.S. Park, D.K. Harshman, A.M. Nicolini, J.-Y. Yoon, Paper microfluidic extraction and direct smartphone-based identification of pathogenic nucleic acids from field and clinical samples, RSC Adv. 4 (2014) 11103–11110.
[24] V. Oncescu, D. O'Dell, D. Erickson, Smartphone based health accessory for colorimetric detection of biomarkers in sweat and saliva, Lab Chip 13 (2013) 3232–3238.
[25] S.K.J. Ludwig, C. Tokarski, S.N. Lang, L.A. van Ginkel, H. Zhu, A. Ozcan, et al., Calling biomarkers in milk using a protein microarray on your smartphone, PLoS One 10 (2015) e0134360.
[26] T.S. Park, W. Li, K.E. McCracken, J.-Y. Yoon, Smartphone quantifies Salmonella from paper microfluidics, Lab Chip 13 (2013) 4832–4840.
[27] Z. Geng, X. Zhang, Z. Fan, X. Lv, Y. Su, H. Chen, Recent progress in optical biosensors based on smartphone platforms, Sensors 17 (2017) 2449.
[28] H. Yu, Y. Tan, B.T. Cunningham, Smartphone fluorescence spectroscopy, Anal. Chem. 86 (2014) 8805–8813.
[29] Z. Rong, Q. Wang, N. Sun, X. Jia, K. Wang, R. Xiao, et al., Smartphone-based fluorescent lateral flow immunoassay platform for highly sensitive point-of-care detection of Zika virus nonstructural protein 1, Anal. Chim. Acta 1055 (2019) 140–147.
[30] J. Li, Y. Sun, C. Chen, T. Sheng, P. Liu, G. Zhang, A smartphone-assisted microfluidic chemistry analyzer using image-based colorimetric assays for multi-index monitoring of diabetes and hyperlipidemia, Anal. Chim. Acta 1052 (2019) 105–112.
[31] E. Aydindogan, E. Guler Celik, S. Timur, Paper-based analytical methods for smartphone sensing with functional nanoparticles: bridges from smart surfaces to Global health, Anal. Chem. 90 (2018) 12325–12333.
[32] D. Vilela, M.C. González, A. Escarpa, Sensing colorimetric approaches based on gold and silver nanoparticles aggregation: chemical creativity behind the assay, Rev. Anal. Chim. Acta 751 (2012) 24–43.
[33] M. Bigas, E. Cabruja, J. Forest, J. Salvi, Review of CMOS image sensors, Microelectron. J. 37 (2006) 433–451.
[34] Y. Zhao, M. Yang, Q. Fu, H. Ouyang, W. Wen, Y. Song, et al., A nanozyme- and ambient light-based smartphone platform for simultaneous detection of dual biomarkers from exposure to organophosphorus pesticides, Anal. Chem. 90 (2018) 7391–7398.
[35] Y. Li, P. Yang, N. Lei, Y. Ma, Y. Ji, C. Zhu, et al., Assembly of DNA-templated bioluminescent modules for amplified detection of protein biomarkers, Anal. Chem. 90 (2018) 11495–11502.
[36] S.K. Vashist, E. Marion Schneider, R. Zengerle, F. von Stetten, J.H.T. Luong, Graphene-based rapid and highly-sensitive immunoassay for C-reactive protein using a smartphone-based colorimetric reader, Biosens. Bioelectron. 66 (2015) 169–176.
[37] L.-J. Wang, Y.-C. Chang, R. Sun, L. Li, A multichannel smartphone optical biosensor for high-throughput point-of-care diagnostics, Biosens. Bioelectron. 87 (2017) 686–692.
[38] D. Zhang, Y. Lu, Q. Zhang, L. Liu, S. Li, Y. Yao, et al., Protein detecting with smartphone-controlled electrochemical impedance spectroscopy for point-of-care applications, Sens. Actuators B Chem. 222 (2016) 994–1002.
[39] K. Mahato, P. Chandra, Paper-based miniaturized immunosensor for naked eye ALP detection based on digital image colorimetry integrated with smartphone, Biosens. Bioelectron. 128 (2019) 9–16.
[40] J.-Y. Huang, H.-T. Lin, T.-H. Chen, C.-A. Chen, H.-T. Chang, C.-F. Chen, Signal amplified gold nanoparticles for cancer diagnosis on paper-based analytical devices, ACS Sens. 3 (2018) 174–182.
[41] F.B. Barlas, E. Aydindogan, M. Arslan, S. Timur, Y. Yagci, Gold nanoparticle conjugated poly(p-phenylene-β-cyclodextrin)-graft-poly(ethylene glycol) for theranostic applications, J. Appl. Polym. Sci. 136 (2019) 47250.
[42] A.C. Templeton, J.J. Pietron, R.W. Murray, P. Mulvaney, Solvent refractive index and core charge influences on the surface plasmon absorbance of alkanethiolate monolayer-protected gold clusters, J. Phys. Chem. B 104 (2000) 564–570.
[43] N.T.K. Thanh, Z. Rosenzweig, Development of an aggregation-based immunoassay

for anti-protein a using gold nanoparticles, Anal. Chem. 74 (2002) 1624–1628.
[44] U. Kreibig, L. Genzel, Optical absorption of small metallic particles, Surf. Sci. 156 (1985) 678–700.
[45] A.K. Trilling, J. Beekwilder, H. Zuilhof, Antibody orientation on biosensor surfaces: a minireview, Analyst 138 (2013) 1619–1627.
[46] H.K. Hunt, A.M. Armani, Label-free biological and chemical sensors, Nanoscale 2 (2010) 1544–1559.
[47] C.A. Schneider, W.S. Rasband, K.W. Eliceiri, NIH Image to ImageJ: 25 years of image analysis, Nat. Methods 9 (2012) 671–675.
[48] Q. Xu, S. Du, G.-d. Jin, H. Li, X.Y. Hu, Determination of acetamiprid by a colorimetric method based on the aggregation of gold nanoparticles, Microchimica Acta 173 (2011) 323–329.
[49] X. Wang, R. Niessner, D. Knopp, Magnetic bead-based colorimetric immunoassay for aflatoxin B1 using gold nanoparticles, Sensors 14 (2014) 21535–21548.
[50] L. Zhou, J.A. Rui, S.B. Wang, S.G. Chen, Q. Qu, The significance of serum AFP cut-off values, 20 and 400 ng/mL in curatively resected patients with hepatocellular carcinoma and cirrhosis might be of difference, Hepato-Gastroenterology 59 (2012) 840–843.
[51] F. Weiland, K. Fritz, M.K. Oehler, P. Hoffmann, Methods for identification of CA125 from ovarian cancer ascites by high resolution mass spectrometry, Int. J. Mol. Sci. 13 (2012) 9942–9958.
[52] M. Wu, H. Liu, Z. Liu, C. Liu, A. Zhang, N. Li, Analysis of serum alpha-fetoprotein (AFP) and AFP-L3 levels by protein microarray, J. Int. Med. Res. 46 (2018) 4297–4305.
[53] M. Felder, A. Kapur, J. Gonzalez-Bosquet, S. Horibata, J. Heintz, R. Albrecht, et al., MUC16 (CA125): tumor biomarker to cancer therapy, a work in progress, Mol. Cancer 13 (2014) 129.
[54] M. Sajid, A.-N. Kawde, M. Daud, Designs, formats and applications of lateral flow assay: a literature review, 19 (2015) 689–705.
[55] G.A. Posthuma-Trumpie, J. Korf, A. van Amerongen, Lateral flow (immuno)assay: its strengths, weaknesses, opportunities and threats. A literature survey, Anal. Bioanal. Chem. 393 (2009) 569–582.